LIVER SEGMENTATION BASED ON DEFORMABLE REGISTRATION AND MULTI-LAYER SEGMENTATION

Hossein Badakhshannoory and Parvaneh Saeedi

School of Engineering Science, Simon Fraser University
Burnaby, BC, Canada
{hba14, psaeedi}@sfu.ca

ABSTRACT

This paper describes a semi-automatic algorithm for extracting liver masks of CT scan volumes. The proposed method relies on two types of information: liver's shape and its intensity characteristics. Here the liver shape information is retained by measuring the shape similarities between consecutive slices of the liver's CT scans. This is done through a deformable registration scheme. The liver intensity is utilized by a multi-layer image segmentation algorithm that emphasizes on the true boundaries of the liver. The proposed algorithm is tested for MICCAI 2007 grand challenge workshop dataset. The average results for volumetric overlap error and relative volume difference is 11.12% and 2.21% respectively.

***Index Terms*—** Liver segmentation, 3D organ reconstruction, deformable registration, mean shift segmentation

1. INTRODUCTION

Planning is an important part of computer assisted minimally invasive surgeries that is done prior to the surgery. It involves preparing a 3D model of the organ under surgery and its surroundings in the patient's body to provide the surgeon with a better understanding of the patient specific anatomy of the surgical site. This 3D model is based on patient's image data that could be acquired from different modalities such as Magnetic Resonance Imaging (MRI), Computed Tomography (CT) or Ultrasound Imaging. The 3D reconstruction of the organ model and its surrounding generally requires various segmentation/extraction algorithms that are applied on the pre-operative scans. A survey of segmentation methods for computer assisted surgery can be found in [1]. Liver is one of the most common human organs that undergoes minimally invasive surgeries and therefore liver segmentation/extraction with least amount of user interaction from pre-operative scans could highly reduce the surgery planning time.

In this paper an algorithm is proposed that does not rely on any training dataset. This approach relies on both the intensity and liver shape information of the CT slices. It is novel in the way that it incorporates the liver shape similarity between consecutive slices by the use of deformable registration. Moreover through a multi-layer segmentation approach true boundaries of the liver regions are detected. Any active contour based method can be added as a fine tuning post processing in cooperation with the proposed algorithm.

1.1. Previous Work

Several methods are proposed in the literature for segmentation of the liver. Some such as [2, 3, 4] use active contours to find liver boundaries. Although effective, they don't take advantage of the shape similarities between the consecutive slices of a liver volume. Some methods use segmentation results of other structures/organs such as ribs in the image as positional reference or limiting boundaries for liver segmentation [5, 6]. The method in [6] utilizes the liver data from previous slices that have been processed by the algorithm. This method however does not exploit the shape similarities between consecutive slices. Other methods such as those based on statistical shape models [7, 8, 9] rely on a training dataset of liver volumes. The performance of these methods is dependent on the type and the number of volumes in the training set. Also there are texture-based classification techniques that do not take advantage of the liver shape information along with intensity information of the liver [10].

The rest of the paper is organized as follows; Section 2 describes the proposed algorithm in details. Section 3 reviews the performance related issues and quantitative results of the system and conclusions are presented in Section 4.

2. PROPOSED METHOD

This paper describes a semi-automatic algorithm for extracting the human liver masks from the CT scan volume of the abdominal area. Although the method is described as semi-automatic, the amount of user interaction is very minor. Inputs to the algorithm are images of one abdominal CT scan volume and one manually identified mask of the liver from a middle slice of the volume in which the liver area is near to its largest size. The output of the algorithm is a set of liver masks for all the remaining slices of the volume. The algorithm starts from one of the middle slices whose liver mask is provided in the input set. It processes input slices in two batches. Both two batches start from the middle slice but one moves in the proximal direction towards the head and the other in the direction towards the feet. In every step, the liver mask of the slice number $i-1$ (previous step's slice) is manipulated to form the liver mask for slice number i (current slice). Such order in processing is held until the last slice in each proximal direction is visited and its liver mask extracted.

Fig. 1 displays the main stream of operations for the proposed method. Details of each process are described next.

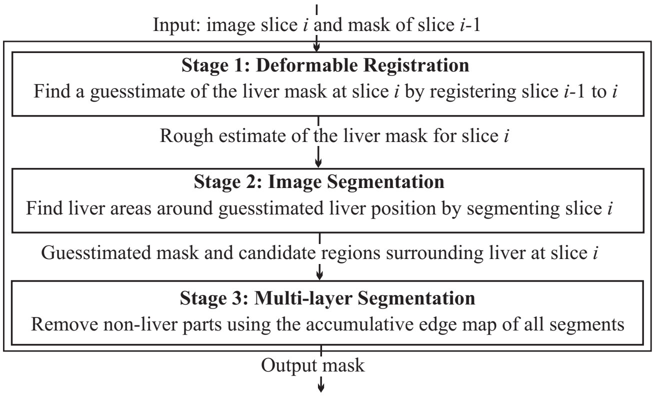

Fig. 1. Order of operations for slice i.

2.1. Stage 1: Deformable Registration

In this stage, shape changes are estimated and tracked from image slice $i-1$ to image slice i. These changes are then applied on the liver mask of slice $i-1$ to form a guesstimate of liver mask for slice i. This operation is done as following:

1. The image of the slice $i-1$ is registered with the image of slice i. Registration is performed using Drop software, which registers using non-rigid registration based on discrete labeling and linear programming [11, 12]. Here the output is a deformation field.

2. The estimated deformation field projects mask points of slice $i-1$ onto their new locations at slice i. Since the transformation transfers integer locations to non-integer locations, the nearest neighbor scheme is used to estimate new transformed locations.

3. The rounding error from nearest neighbor scheme manifests itself by a number of scattered undefined/empty points inside new masks. A morphological closing is applied to close empty points on the new mask.

Due to the fact that often each liver dataset contains sudden and large changes including additive connected or isolated pieces from one slice to the next, the results of this operation cannot account for all changes that exist between two consecutive slices. Hence, these results are basically a rough estimate of the liver's profile at slice i, which might not necessarily cover the entire actual liver region. The result of this stage for a typical case is shown in Fig.2-b. Fig. 2-a shows the initial mask for slice $i-1$.

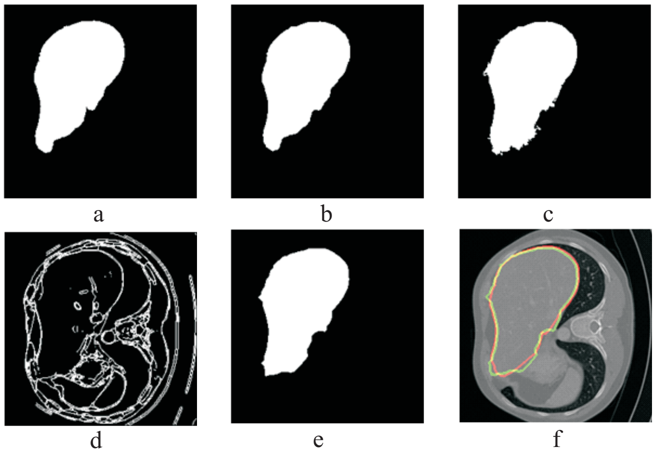

Fig. 2. Intermediate image results at different Stages.

2.2. Stage 2: Image Segmentation

After having a guesstimate of the liver mask at slice i, the algorithm inspects those regions that are newly appeared in the slice i compared to slice $i-1$. For this, first the liver image is segmented using the mean shift segmentation algorithm [13]. A set of parameters is chosen for the segmentation so that regions with texture similarity, regardless of the regions' noise level, are segmented into the same class.

Using results of the segmentation, all image regions that are physically connected to each other and have overlaps with the mask guesstimate of the liver, are connected to each other to generate an updated liver mask definition. This step is intended for identifying and admitting all liver regions that just appeared in slice i and were not present in slice $i-1$. It must be noted that, organs and tissues in close proximity of the liver with similar textures to the liver could be wrongly added to the liver mask at this stage. A typical result for this stage is shown in Fig. 2-c.

2.3. Stage 3: Multi-layer Segmentation

This stage removes those regions that were wrongly identified as liver and added to the mask. For this purpose, a boundary that surrounds the liver region at slice i is required. To estimate such boundary an edge map that contains all edges of the liver is utilized using a multi-layer segmentation technique. In this technique the image of slice i is segmented with the mean shift algorithm several times using a range of parameters. The boundary edges of all segmented slices are then extracted. The extracted edges are added together to form an accumulative edge map (AEM). The AEM highlights more dominant edges such as liver external boundaries which are less sensitive to the parameter setting of the segmentation algorithm. The contrast of AEM is enhanced using Log transform. The enhanced AEM is thresholded (computed automatically) to form an Enhanced Edge Map (EEM) that contains only liver's boundary edges. If the edge map of a segmented image is called $EMSI$ and s represents the segmentation parameters for the mean shift algorithm, the above operation can be described by:

$$AEM = \sum_{s} EMSI \tag{1}$$

$$EEM(x,y) = \begin{cases} 1 & Log(AEM(x,y)) > Thresh \\ 0 & \text{otherwise} \end{cases} \tag{2}$$
$$\text{Where:} \quad Thresh = \frac{max(Log(AEM)) - min(Log(AEM))}{2}$$

A sample result for generating the EEM is shown in Fig. 2-d. EEM is then subtracted from the output of segmentation operation at Stage 2 (Fig. 2-c) to separate the liver from non-liver regions. The result for this stage is shown in Fig. 2-e. The results of proposed method and the manual extraction are overlaid on a sample slice as shown in Fig. 2-f.

2.4. Refinement of Non-single Piece Liver Masks

Due to anatomical features of the liver, often its cross sections consist of two or more pieces. When processing such slices, the proposed algorithm creates only a one piece mask for the largest piece of the liver. In order to identify and add the missing secondary pieces of the liver to the mask, a supplementary process is required.

In the supplementary process the system first returns to the starting slice (middle slice, say index $i-1$). The liver mask for this slice will be transformed onto the slice i using the deformable transformation scheme proposed in Stage 1. Comparing results of this transformation with the actual mask of slice i (found by running Stages 1 to 3) the algorithm determines whether there is any large piece of the expected mask missing. If not, the supplementary process moves to the slice i and uses its mask as the ground truth for slice $i+1$. If however one or more pieces of the expected mask are missing, the algorithm has estimated the guesstimates of the missing mask pieces (through the subtraction) in slice i. The following two conditions must be satisfied for each of the secondary pieces to be examined as a potential missing mask piece.

1. They had been part of liver mask in slice $i-1$, and
2. Its area must be at least 10% (an empirical threshold) of the previously calculated mask area at slice i.

The mask identification process (Stages 2 to 3) then will be applied to all secondary pieces that have satisfied the above two conditions to fine estimate each secondary mask piece. Once all pieces are estimated, they will be added to the mask of slice i and the process continues by finding all secondary pieces of slice $i+1$ using the updated mask of slice i as the ground truth. This process is performed for all slices of the volume in two batches on the two sides of the middle slice.

Some results are shown in Fig. 3. Figs. 3-a and -b display results for non-single pieces and 3-c and 3-d for dark slices. Figs. 3-h and 3-i depict examples of less than perfect results.

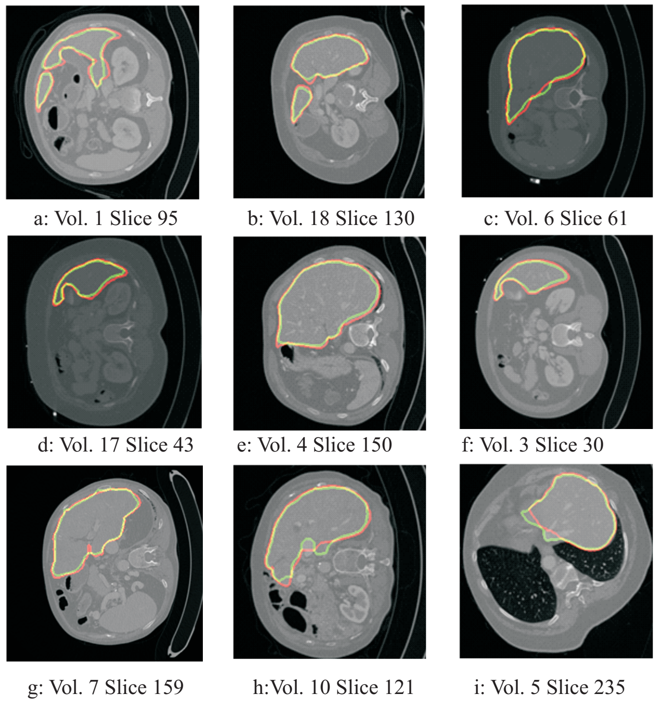

Fig. 3. Sample results from the training volumes of MICCAI 2007 dataset (red: ground truth, green: boundaries by the proposed algorithm, yellow: their overlaps).

3. RESULTS AND DISCUSSION

In order to evaluate the results of the proposed method, the datasets and evaluation metrics from MICCAI 2007 grand challenge workshop [14] are adopted. The dataset includes 20 training and 10 test volumes. The results for the test volumes are shown in Table 1. The definition of the metrics used can be found in [14].

The average runtime for extracting one liver mask for this algorithm is 30 seconds using MATLAB 7.6.0.324 environment on a PC with an Intel Core 2 Duo (2 GHz) processor.

The proposed method is similar to the methods in [6, 10] in the way that it does not require training data. The results of the proposed method are superior compared to the result of [6, 10] in terms of all metrics. It must be noted that the algorithm does not outperform the method proposed by [7, 8, 9] due to the fact that these algorithms rely on a training set and ours does not.

It is also important to mention that the performances of [7, 8, 9] are dependent on the number and the type of training data available for segmenting the liver from patients CT scan. Due to diversity of liver shape and size, performance of such method could differ from patient to patient.

Table 1. Quantitative results for the proposed method.

Data set No.	Vol overlap error%	Score	Ave symm diff%	Score	Ave symm surface dist [mm]	Score	RMS symm surface dist [mm]	Score	Max symm surface dist [mm]	Score	Total
1	10.08	60.63	-1.99	89.39	1.54	61.62	2.53	64.86	17.96	76.36	70.57
2	11.00	57.03	-3.57	81.02	1.90	52.58	4.13	42.67	40.95	46.11	55.88
3	12.18	52.41	-9.63	48.80	4.72	0.00	9.38	0.00	50.44	33.63	26.97
4	10.52	58.90	1.66	91.19	2.03	49.18	3.94	45.22	27.34	64.03	61.70
5	12.95	49.40	0.50	97.33	2.81	29.79	6.69	7.14	73.15	3.75	37.48
6	11.57	54.80	-4.03	78.59	1.91	52.15	3.32	53.88	24.28	68.05	61.49
7	9.55	62.71	2.30	87.77	2.21	44.83	5.67	21.23	47.68	37.26	50.76
8	9.68	62.18	0.99	94.74	2.25	43.73	4.58	36.33	34.81	54.20	58.24
9	8.34	67.41	-2.18	88.42	1.01	74.82	1.85	74.27	20.83	72.59	75.50
10	15.33	40.11	-6.18	67.11	3.55	11.25	6.66	7.57	37.20	51.06	35.42
Mean	11.12	56.26	-2.21	82.44	2.39	41.99	4.87	35.32	37.47	50.70	53.40

4. CONCLUSIONS

In this paper an algorithm for extracting liver masks of CT scan volumes from abdominal area is proposed. The algorithm is semi-automatic since it requires one accurate liver mask from a middle slice of the processed volume. This algorithm is novel in the way that instead of relying on training dataset to estimate liver shape (which can be dependent upon the number and the type of training volumes), it capitalizes on gradual shape changes on consecutive CT slices. Changes on consecutive slices are estimated by deformable registration. A multi-layer segmentation algorithm is incorporated to acquire border points of the liver. The quantitative segmentation results show an overall improvement of 9.14% in the volumetric overlap error and 2.3% in the relative volume difference comparing to the results by [6]. The algorithm generates results that are better in the maximum symmetric distance by 6.34mm, the average symmetric surface distance by 1.72mm and the RMS symmetric surface distance by 2.83mm comparing to the similar non-training based technique in [6].

5. REFERENCES

[1] Z. Yaniv and K. Cleary, "Image-guided procedures: A review," *Comput. Aided Interventions and Med. Robotics, Imaging Science and Inf. Systems Center, Dpt. of Radiology, Georgetown University Med. Center, Tech. Rep.*, Apr 2006.

[2] A. Linney A. Evans, T. Lambrou and A. Todd-Pokropek, "Automatic segmentation of liver using a topology adaptive snake," in *Proc. of the 2nd Int. Conf. Biomed. Eng.*, 2004.

[3] J. F. Garamendi, N. Malpica, J. Martel, and E. Schiavi, "Automatic segmentation of the liver in ct using level sets without edges," in *Proc. of the 3rd Iberian conf. on Pattern Rec. and Img. Analysis, Part I.* 2007, pp. 161–168, Springer-Verlag.

[4] S. Pan and B. M. Dawant, "Automatic 3d segmentation of the liver from abdominal ct images: a level-set approach," *Med. Imaging: Img. Proc.*, vol. 4322, no. 1, pp. 128–138, 2001.

[5] K. Seo, L. C. Ludeman, S. Park, and J. Park, "Efficient liver segmentation based on the spine," in *ADVIS*, 2004, pp. 400–409.

[6] M. Hori A. H. Forouzan, R. A. Zoroofi and Y. Sato, "Liver segmentation by intensity analysis and anatomical information in multi-slice ct images," *Proc. of Int. Journal CARS*, vol. 4, pp. 287–297, Mar 2009.

[7] L. Soler, H. Delingette, G. Malandain, J. Montagnat, N. Ayache, C. Koehl, O. Dourthe, B. Malassagne, M. Smith, D. Mutter, and J. Marescaux, "Fully automatic anatomical, pathological, and functional segmentation from ct scans for hepatic surgery.," *Comp. Aided Surg.*, vol. 6, no. 3, pp. 131–142, 2001.

[8] D. Kainmuller, T. Lange, and H. Lamecker, "Shape constrained automatic segmentation of the liver based on a heuristic intensity model," in *Proc. MICCAI Workshop 3D Segmentation in the Clinic: A Grand Challenge*, 2007, pp. 109–116.

[9] H. P. Meinzer T. Heimann and I. Wolf, "A statistical deformable model for the segmentation of liver ct volumes," in *Proc. MICCAI Workshop 3D Segmentation in the Clinic: A Grand Challenge*, 2007, pp. 161–166.

[10] R. Susomboon, D. Raicu, and J. Furst, "A hybrid approach for liver segmentation," in *Proc. MICCAI Workshop 3D Segmentation in the Clinic: A Grand Challenge*, 2007, pp. 151–160.

[11] B. Glocker, N. Komodakis, G. Tziritas, N. Navab, and N. Paragios, "Dense image registration through mrfs and efficient linear programming," *Med. Img. Anal.*, vol. 12, no. 6, pp. 731–741, 2008.

[12] N. Komodakis, G. Tziritas, and N. Paragios, "Fast, approximately optimal solutions for single and dynamic mrfs," in *CVPR*, 2007, pp. 1–8.

[13] P. Meer D. Comaniciu, "Mean shift: A robust approach toward feature space analysis," *IEEE Trans. PAMI*, vol. 24, no. 5, pp. 603–619, 2002.

[14] B. van Ginneken, T. Heimann, and M. Styner, "3d segmentation in the clinic: A grand challenge," *MICCAI, Img. Sciences Inst., University Med. Center Utrecht*, pp. 7–15, 2007.